



# **Improved Diagnosis and Fault Tolerant Control Wind Power System Using Sliding Mode Observer**

N Boumalha<sup>1\*</sup>, D Kouchih<sup>2</sup>, MS Boucherit<sup>1</sup>, M Tadjine<sup>1</sup>

<sup>1</sup>Process Control Laboratory, 10 Avenue H. Badi BP 182 Automatic control department, ENP Alger, Algeria

<sup>2</sup>Electronic Department, University SaadDahlab, Blida, Algeria

**ABSTRACT:** In this paper, we present a grid-connected wind turbine equipped with double-fed induction generator directly connected to the grid in the stator side and interconnected via a power converter in the rotor side. Then we present a fault tolerant control (FTC) based on sliding mode observer for stator winding fault of DFIG. We develop an algorithm that allows the passage from nominal controllers designed for healthy condition, to robust controllers designed for faulty condition. Simulation results have shown good performances of the system under these proposed approach strategies.

**KEYWORDS:** Wind turbine; Doublyfed induction generator; Sliding mode observer; Inter-turn short-circuit; diagnosis; Fault tolerant control

## **I. INTRODUCTION**

To produce electrical energy using a wind energy conversion system (WECS), various control strategies have been developed in the literature [1]. All this strategies have the goal to bring down the cost of electrical energy produced by the WECS and to convergethe system for operating at unity power factor. The field oriented control strategy (FOC) has attracted much attention in the past fewdecades but it suffers from the problem of the machine parameters variations, which comes to compromise the robustness of the control device[2]. Indeed, the PI regulators coefficients used in FOC strategy, are directly calculated according to the parameters machine what entrain a poor robustness vs parameters variations [3,4]. Vector control methods for DFIG have been addressed in some literatures [5]. DFIG is essentially a wound rotor induction machine in combination with bi-directional back to back PWM converters, in which the stator windings are directly connected to the grid and the rotor windings are injected with variable voltages at slip frequency. The rotor side converter is used to control the rotor injection voltages and the grid side converter is used to maintain a constant voltage on the DC link voltage. A typical configuration of a wind turbine DFIG is shown in Figure1. Decoupled d-q vector control is a common control strategy of wind turbine DFIG, which is mainly realized by controlling the rotor side converter. This controller isconsisted of two stages with the first stage for active and reactive power control and the second stage for d and q control signals through this two-stage controller, activepower and reactive power can be controlled separatelyaccording to their setting points. To generate the maximumpower, the active power setting point should be adjustedwith the rotor speed according to maximum powerextraction control strategy. This control strategy is implemented in thiswork to control the rotor voltage signals and give thereference values of the active and reactive power when theoperating condition changes. The fault detection andlocalization unit detects the occurrence of fault anddetermines its nature. This can be realized by analyzing thechange of the stator or rotor resistance and then take theappropriate decision: accept the default or stop the machineand execute a curative maintenance. This paper proposes anovel adaptive estimation method developed, to design anadaptive sliding mode observer, parameters changes can betacked by using this method. Through adjusting the errorbetween the reference and adjustable models by slidingmode algorithm, the estimated rotor resistance can beobtained. So, the proposed FTC is a combination betweenan active and passive FTC. The advantage of this FTC is that when the fault is not tolerant an alarm signal willindicate that the operator's intervention is necessary. TheFTC control method is implemented by Matlab/simulinkand several steady and dynamic experimental results are given [6].

The schema of the device studied is given in Figure 1.

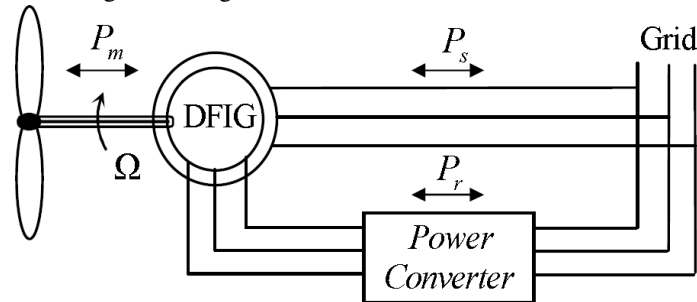


**Figure 1: Configuration of a DFIG wind turbine system.**

## II. DFIG MODELING

### 2.1.1. Model in a-b-c Coordinate Reference Frame

In the stator reference frame ( $\alpha$ - $\beta$ s), the mechanical/electrical energy conversion process is described by the equations of DFIG are defined by:

$$\begin{cases} V_{\alpha s} = R_s \cdot i_{\alpha s} + \frac{d\psi_{\alpha s}}{dt} \\ V_{\beta s} = R_s \cdot i_{\beta s} + \frac{d\psi_{\beta s}}{dt} \\ V_{\alpha r} = R_r \cdot i_{\alpha r} + \frac{d\psi_{\alpha r}}{dt} + \omega_r \psi_{\beta r} \\ V_{\beta r} = R_r \cdot i_{\beta r} + \frac{d\psi_{\beta r}}{dt} + \omega_r \psi_{\alpha r} \end{cases} \quad (1)$$

The equations of stator and rotor flux are given as follows:

$$\begin{cases} \psi_{\alpha s} = L_s \cdot i_{\alpha s} + M_{sr} \cdot i_{\alpha r} \\ \psi_{\beta s} = L_s \cdot i_{\beta s} + M_{sr} \cdot i_{\beta r} \\ \psi_{\alpha r} = L_r \cdot i_{\alpha r} + M_{rs} \cdot i_{\alpha s} \\ \psi_{\beta r} = L_r \cdot i_{\beta r} + M_{rs} \cdot i_{\beta s} \end{cases} \quad (2)$$





# International Journal of Advanced Research in Electrical, Electronics and Instrumentation Engineering

(An ISO 3297: 2007 Certified Organization)

Website: [www.ijareeie.com](http://www.ijareeie.com)

Vol. 6, Issue 11, November 2017

With

$$A_{11} = \begin{bmatrix} \left( \frac{-1}{\sigma\tau_s} \frac{L_m^2}{\tau_s\sigma L_s L_r} \right) & 0 \\ 0 & \left( \frac{-1}{\sigma\tau_s} \frac{L_m^2}{\tau_s\sigma L_s L_r} \right) \end{bmatrix}$$

$$A_{12} = \begin{bmatrix} \frac{L_m}{\tau_s\sigma L_s L_r} & \frac{wL_m}{\sigma L_s L_r} \\ \frac{wL_m}{\sigma L_s L_r} & \frac{L_m}{\tau_s\sigma L_s L_r} \end{bmatrix}$$

$$A_{21} = \begin{bmatrix} \frac{L_m}{\tau_s} & 0 \\ 0 & \frac{L_m}{\tau_s} \end{bmatrix}, \quad A_{22} = \begin{bmatrix} \frac{-1}{\tau_s} & -w \\ w & \frac{-1}{\tau_s} \end{bmatrix}$$

$$B_{11} = \begin{bmatrix} \frac{1}{\sigma L_s} & 0 \\ 0 & \frac{1}{\sigma L_s} \end{bmatrix}, \quad B_{12} = \begin{bmatrix} \frac{-L_m}{\sigma L_s L_r} & 0 \\ 0 & \frac{-L_m}{\sigma L_s L_r} \end{bmatrix}$$

$$B_{21} = \begin{bmatrix} 0 & 0 \\ 0 & 0 \end{bmatrix}, \text{ and } B_{22} = \begin{bmatrix} 1 & 1 \\ 1 & 1 \end{bmatrix}$$

And  $\sigma = 1 - L_m^2 (L_s L_r), w = p\Omega_{mec}$

Where,  $R_s$  and  $R_r$  are the stator and rotor resistance, respectively.  $L_s, L_r$  and  $L_m$  are the stator and rotor full inductance, the magnetization inductance, respectively.

The electromagnetic torque equation becomes[7]:



# International Journal of Advanced Research in Electrical, Electronics and Instrumentation Engineering

(An ISO 3297: 2007 Certified Organization)

Website: [www.ijareeie.com](http://www.ijareeie.com)

Vol. 6, Issue 11, November 2017

$$C_e = \frac{3}{2} p \frac{L_m}{L_r} (\Phi_{ar} i_{\beta s} - \Phi_{\beta r} i_{\alpha s}) \quad (5)$$

### III. VECTOR CONTROL OF DFIG

In order to establish a vector control of DFIG, we recall here its modelling in the Park frame. The equations of the stator voltages and rotor of the DFIG are defined by equation (1 and 2).

$$\begin{cases} V_{ds} = R_s \cdot i_{\alpha s} + \frac{d}{dt} [\psi_{ds}] - \omega_s \psi_{qs} \\ V_{qs} = R_s \cdot i_{qs} + \frac{d}{dt} [\psi_{qs}] + \omega_s \psi_{ds} \\ V_{dr} = R_r \cdot i_{dr} + \frac{d}{dt} [\psi_{dr}] - \omega_r \psi_{qr} \\ V_{qr} = R_r \cdot i_{qr} + \frac{d}{dt} [\psi_{qr}] + \omega_r \psi_{dr} \end{cases} \quad (8)$$

The equations of stator and rotor flux are given as follows [8]:

$$\begin{cases} \psi_{ds} = L_s \cdot i_{ds} + M_{sr} \cdot i_{dr} \\ \psi_{qs} = L_s \cdot i_{qs} + M_{sr} \cdot i_{qr} \\ \psi_{dr} = L_r \cdot i_{dr} + M_{rs} \cdot i_{ds} \\ \psi_{qr} = L_r \cdot i_{qr} + M_{rs} \cdot i_{qs} \end{cases} \quad (9)$$

The electromagnetic torque can be expressed by:

$$C_{em} = p \frac{M_{sr}}{L_r} (\psi_{ds} I_{qr} - \psi_{qs} I_{dr}) \quad (10)$$

The principle of vector control with stator flux oriented of the DFIG is shown in Figure 3. The stator flux vector will be aligned on the 'd' axis and the stator voltage vector on the 'q' axis, this last constraint is favorable to obtain a simplified control model.

# International Journal of Advanced Research in Electrical, Electronics and Instrumentation Engineering

(An ISO 3297: 2007 Certified Organization)

Website: [www.ijareeie.com](http://www.ijareeie.com)

Vol. 6, Issue 11, November 2017

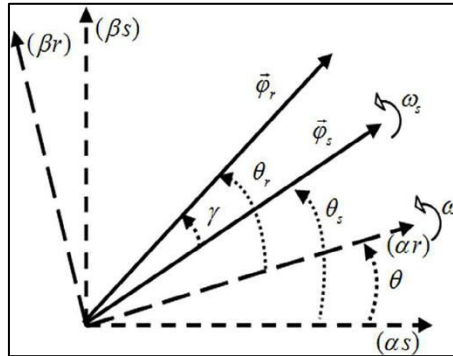


Figure3: Stator voltage and flux vectors in the axis system.

The electromagnetic torque equation becomes:

$$C_{em} = p \frac{M_{sr}}{L_r} \psi_{ds} I_{qr} \quad (11)$$

Assuming the grid is connected to the DFIG is stable, the flux  $\psi_{ds}$  becomes constant. The choice of this reference makes the electromagnetic torque and the active power produced by the machine. Dependent only of 'q' axis rotor current components [9].

In the same reference, the tensions can obtain by equations:

$$\begin{cases} V_{ds} = 0 \\ V_{qs} = V_s = \omega_s \psi_{ds} = \omega_s \psi_s \end{cases} \quad (12)$$

Using the previous simplifications, the stator flux equations can be written by:

$$\begin{cases} \psi_s = L_s I_{ds} + M_{sr} I_{dr} \\ 0 = L_s I_{qs} + M_{sr} I_{qr} \end{cases} \quad (13)$$

The equations linking the stator currents to the rotor currents are deduced below:

$$\begin{cases} I_{ds} = \frac{\psi_s}{L_s} - \frac{M_{sr}}{L_s} I_{dr} \\ I_{qr} = -\frac{M_{sr}}{L_s} I_{qs} \end{cases} \quad (14)$$

In park reference, the stator active and reactive power of an induction machine are expressed as:

$$\begin{cases} P_s = V_{ds} I_{ds} + V_{qs} I_{qs} \\ Q_s = V_{qs} I_{ds} + V_{ds} I_{qs} \end{cases} \quad (15)$$

# International Journal of Advanced Research in Electrical, Electronics and Instrumentation Engineering

(An ISO 3297: 2007 Certified Organization)

Website: [www.ijareeie.com](http://www.ijareeie.com)

Vol. 6, Issue 11, November 2017

By replace the equation (14) and (15) in (16), the active and reactive powers can be written as a function of rotor currents as follows [10-12]:

$$\begin{cases} P_s = -V_s \frac{M_{sr}}{L_s} I_{qr} \\ Q_s = \frac{V_s \psi_s}{L_s} - \frac{V_s M_{sr}}{L_s} I_{dr} \end{cases} \quad (16)$$

The rotor voltages can be written as a function of rotor currents as follows:

$$\begin{cases} V_{dr} = R_r I_{dr} + \left( L_r - \frac{M_{sr}^2}{L_s} \right) \frac{d}{dt} I_{dr} + g \omega_s \left( L_r - \frac{M_{sr}^2}{L_s} \right) I_{qr} \\ V_{qr} = R_r I_{qr} + \left( L_r - \frac{M_{sr}^2}{L_s} \right) \frac{d}{dt} I_{qr} + g \omega_s \left( L_r - \frac{M_{sr}^2}{L_s} \right) I_{dr} + g \omega_s \frac{M_{sr} V_s}{\omega_s L_s} \end{cases} \quad (17)$$

After applying the Laplace transformation to the equations (16) and (17) gives:

$$\begin{cases} V_{dr} = \left[ R_r + \left( L_r - \frac{M_{sr}^2}{L_s} \right) S \right] I_{dr} - g \omega_s \left( L_r - \frac{M_{sr}^2}{L_s} \right) I_{qr} \\ V_{qr} = \left[ R_r + \left( L_r - \frac{M_{sr}^2}{L_s} \right) S \right] I_{qr} + g \omega_s \left( L_r - \frac{M_{sr}^2}{L_s} \right) I_{dr} + g \omega_s \frac{M_{sr} V_s}{\omega_s L_s} \end{cases} \quad (18)$$

## IV. MODELLING OF DFIG WITH STATOR INTER-TURN FAULT

A DFIG model in a-b-c coordinate reference frame is derived to describe the inter-turn short circuit fault at any level in any single phase of rotor. In this model, the fault position parameter  $f$  is defined as below for three cases that fault occurs in phase 'a', 'b' and 'c', respectively.

$$f_a = [1 \ 0 \ 0]^T, f_b = [0 \ 1 \ 0]^T, f_c = [0 \ 0 \ 1]^T$$

The fault level parameter  $\gamma$  denotes the fraction of the shorted winding.

For modelling this defect, we assume that a number of turns «  $\gamma$  » from among those « a » is shortcircuited. This section of turns short circuit is defined by coefficient «  $\gamma$  » between the number of turns short - circuited and the total number of turns of the phase « a », this coefficient is introduced in the mathematical model governing the operation of the machine, The modeling of the DFIG with fault is to introduce resistance «  $fR$  » in parallel with the turns short circuit in phase infected (Figure 4).

## International Journal of Advanced Research in Electrical, Electronics and Instrumentation Engineering

(An ISO 3297: 2007 Certified Organization)

Website: [www.ijareeie.com](http://www.ijareeie.com)

**Vol. 6, Issue 11, November 2017**

A voltage will be induced in mesh short-circuit, the voltage induced circulating current in the shorted turns called fault current, This latter has a proportional relationship with the fault resistance and induced voltage.

Therefore the inductance and resistance of the faulty phase change and the mutual inductance between this phase and all other windings of the machine will be changed. The new form of the equations of stator voltages is then rewritten as follows [13]:

$$[V_s] = [R_s][I_s] + \frac{d[\psi_s]}{dt}$$

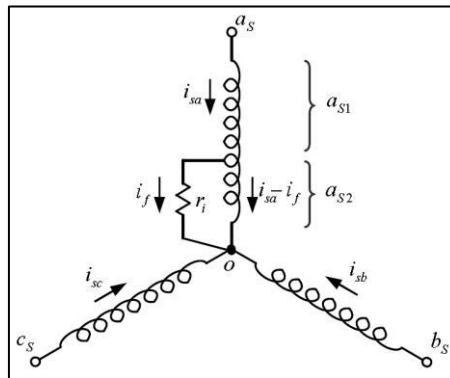


**Figure 4: Stator winding configuration with the inter-turn short circuit fault in phase 'a'.**

The stator resistance matrix can be rewritten as follows:

$$[R_s] = \begin{bmatrix} (1-\gamma)R_s & 0 & 0 & \gamma R_s \\ 0 & R_s & 0 & 0 \\ 0 & 0 & R_s & 0 \\ 0 & 0 & 0 & \gamma R_s \end{bmatrix} \quad (19)$$

However, we keep the matrix of stator voltages unchanged [14-16].

If we mean by  $\langle \gamma \rangle$  fraction of the number of shorted turns of phase « a », then we have a healthy portion of a fraction  $1-\gamma$  of turns and we suppose the phases "b" and "c" healthy. We will have the new inductance stator matrix following:



# International Journal of Advanced Research in Electrical, Electronics and Instrumentation Engineering

(An ISO 3297: 2007 Certified Organization)

Website: [www.ijareeie.com](http://www.ijareeie.com)

Vol. 6, Issue 11, November 2017

$$[L_{ss}] = L_{fs} \text{diag} [(1-\gamma)11\gamma] + M_s \begin{bmatrix} (1-\gamma)^2 & -\frac{(1-\gamma)}{2} & -\frac{(1-\gamma)}{2} & \gamma(1-\gamma) \\ -\frac{(1-\gamma)}{2} & 1 & -\frac{1}{2} & -\frac{\gamma}{2} \\ -\frac{(1-\gamma)}{2} & -\frac{1}{2} & 1 & -\frac{\gamma}{2} \\ \gamma(1-\gamma) & -\frac{\gamma}{2} & -\frac{\gamma}{2} & \gamma^2 \end{bmatrix} \quad (20)$$

Therefore, the matrix of mutual inductances is:

$$[M_{sr}] = M_s \begin{bmatrix} (1-\gamma)\cos(\theta_r) & (1-\gamma)\cos\left(\theta_r + \frac{2\pi}{3}\right) & (1-\gamma)\cos\left(\theta_r - \frac{2\pi}{3}\right) \\ \cos\left(\theta_r - \frac{2\pi}{3}\right) & \cos(\theta_r) & \cos\left(\theta_r + \frac{2\pi}{3}\right) \\ \cos\left(\theta_r + \frac{2\pi}{3}\right) & \cos\left(\theta_r - \frac{2\pi}{3}\right) & \cos(\theta_r) \\ \gamma\cos(\theta_r) & \gamma\cos\left(\theta_r + \frac{2\pi}{3}\right) & \gamma\cos\left(\theta_r - \frac{2\pi}{3}\right) \end{bmatrix} \quad (21)$$

Rotor inductance matrix remains equal to that of the healthy cases.

## V. SLIDING MODE OBSERVER

Many schemes have been developed to estimate parameter of DFIG from measured terminal quantities. One of these estimation systems are based on sliding mode technique. In order to obtain a better estimation, it is necessary to have dynamic representation based on the stationary ( $\alpha \beta$ ) reference frame. Since machine voltages and currents are measured in a stationary frame, it is also convenient to express these equations in stationary ( $\alpha \beta$ ) reference frame. We use the state-space form using stator currents and rotor fluxes as expressed in the previous section. The idea is that the error between the actual and observed stator currents converges to zero, which guarantees the accuracy of the rotor flux observer. So, we define a sliding surface  $S=[S1 \ S2]$  as to converge to zero the two sliding variables (i.e.  $S1=0, S2=0$ ) [17-20] (Figure 5).

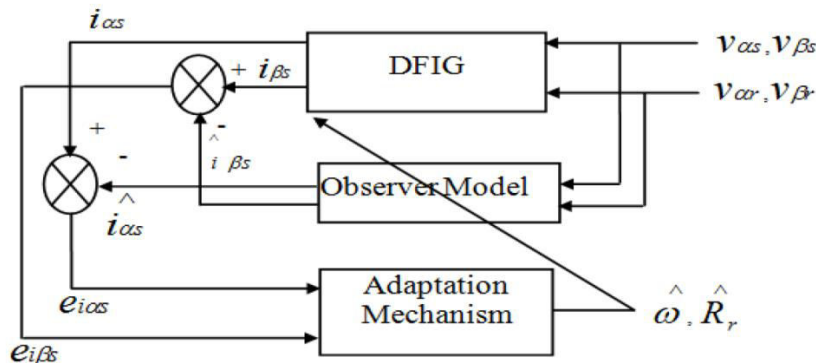


Figure 5: Principle of sliding mode observer.



## International Journal of Advanced Research in Electrical, Electronics and Instrumentation Engineering

(An ISO 3297: 2007 Certified Organization)

Website: [www.ijareeie.com](http://www.ijareeie.com)

Vol. 6, Issue 11, November 2017

The model of the observer is written:

$$\begin{cases} \frac{d\hat{X}}{dt} = \hat{A}\hat{X} + BU + G\text{sign}(Y - \hat{Y}) \\ \hat{Y} = C\hat{X} \end{cases} \quad (22)$$

With

$$X = [i_{\alpha s} \ i_{\beta s} \ \Phi_{\alpha r} \ \Phi_{\beta r}]^t, Y = \begin{pmatrix} i_{\alpha s} \\ i_{\beta s} \end{pmatrix}$$

$$u = [u_{\alpha s} \ u_{\beta s} \ u_{\alpha r} \ u_{\beta r}]^t$$

$$A = \begin{bmatrix} -\left(\frac{R_s}{\sigma L_s} + \left(\frac{R_r L_m^2}{\sigma L_s L_r^2}\right)\right) I & \frac{L_m}{\sigma L_s L_r} \left(\frac{R_r}{L_r} I - \omega J\right) \\ \left(\frac{L_m R_r}{L_r}\right) I & -\left(\frac{R_r}{L_r} I - \omega J\right) \end{bmatrix}$$

$$\hat{A} = \begin{bmatrix} -\left(\frac{R_s}{\sigma L_s} + \left(\frac{R_r L_m^2}{\sigma L_s L_r^2}\right)\right) I & \frac{L_m}{\sigma L_s L_r} \left(\frac{R_r}{L_r} I - \hat{\omega} J\right) \\ \left(\frac{L_m R_r}{L_r}\right) I & -\left(\frac{R_r}{L_r} I - \hat{\omega} J\right) \end{bmatrix}$$

$$B = \begin{bmatrix} \frac{1}{\sigma L_s} I & \frac{L_m}{\sigma L_s L_r} I \\ 0_{2 \times 2} & I \end{bmatrix}, C = \begin{pmatrix} 1 & 0 & 0 & 0 \\ 0 & 1 & 0 & 0 \end{pmatrix}$$

And

$$J = \begin{bmatrix} 0 & -1 \\ 1 & 0 \end{bmatrix}, I = \begin{bmatrix} 1 & 0 \\ 0 & 1 \end{bmatrix}$$

We put

$$a = \frac{1}{\sigma L_s} \left( R_s + R_r \frac{L_m^2}{L_r} \right), b = \sigma L_s L_r, \sigma = 1 - \frac{L_m^2}{L_s L_r}$$

$$I_s = [\text{sign}(S_1) \ \text{sign}(S_2)]^T \text{ and } \begin{cases} x_1 - \hat{x}_1 \\ x_2 - \hat{x}_2 \end{cases}$$

$S_1, S_2$  represent the sliding surfaces.



# International Journal of Advanced Research in Electrical, Electronics and Instrumentation Engineering

(An ISO 3297: 2007 Certified Organization)

Website: [www.ijareeie.com](http://www.ijareeie.com)

Vol. 6, Issue 11, November 2017

The gains:  $q_1, \wedge_1^T, \wedge_2^T, \wedge_3^T, \wedge_4^T, \wedge_5^T$  are calculated to ensure the asymptotic convergence of errors estimation. They are given by:

$$\begin{bmatrix} \wedge_1^T \\ \wedge_2^T \end{bmatrix} = D^{-1} \begin{bmatrix} \delta_1 & 0 \\ 0 & \delta_2 \end{bmatrix}$$

$$D = \frac{1}{(a^2 + (kpx_5)^2)} \begin{bmatrix} a & -kpx_5 \\ kpx_5 & a \end{bmatrix}$$

$$\begin{bmatrix} \wedge_{31} & \wedge_{32} \\ \wedge_{41} & \wedge_{42} \end{bmatrix} = \begin{bmatrix} -c & -px_5 \\ px_5 & -c \end{bmatrix} \begin{bmatrix} q_3 & 0 \\ 0 & q_4 \end{bmatrix} \begin{bmatrix} \delta_1 & 0 \\ 0 & \delta_2 \end{bmatrix} \quad (23)$$

$$\begin{bmatrix} \wedge_{51} \\ \delta_1 \end{bmatrix} \quad \begin{bmatrix} \wedge_{52} \\ \delta_2 \end{bmatrix} = d \begin{bmatrix} x_2 & -x_1 \end{bmatrix}$$

$$\begin{cases} \delta_1 > |e_3|_{\max} \\ \delta_2 > |e_4|_{\max} \end{cases} \text{ and } \begin{cases} q_1 > 0 \\ q_2 > 0 \\ q_3 > 0 \end{cases}$$

The residual signal is calculated as  $r = [Y - \hat{Y}]$  follows, and we define as the detection threshold (lower limit), which is set according to some pre-specified (expected) system performances. The objective is to determine the mechanism adaptation of the speed and the rotor resistance. The structure of the observer is based on the DFIG model in stator reference frame.

The rotor resistance estimation can be written as follows:

$$\hat{R}_r = \int_0^t \lambda \begin{bmatrix} \frac{L_m}{bL_r} (\hat{\Phi}_{ar} \text{sign}e_{i_{as}} + \hat{\Phi}_{\beta r} \text{sign}e_{i_{\beta s}}) \\ -\frac{1}{\sigma L_s} (\hat{i}_{as} \text{sign}e_{i_{as}} + \hat{i}_{\beta s} \text{sign}e_{i_{\beta s}}) \end{bmatrix} dt \quad (24)$$

With:  $\lambda$  is a positive scalar.

## VI. SIMULATION RESULTS

The simulation behaviour of DFIG that we present in this part will help analyze the outputs variables with stator active and reactive power imposition to maximize the developed for both conditions with and without stator interturn short circuit fault applied as a wind turbine generator. The technique presented in the previous sections has been implemented in the MATLAB/simulink. The simulation test involves the wind speed variation and the reactive power reference constant equals to zero, as shown in the Table 1.

# International Journal of Advanced Research in Electrical, Electronics and Instrumentation Engineering

(An ISO 3297: 2007 Certified Organization)

Website: [www.ijareeie.com](http://www.ijareeie.com)

Vol. 6, Issue 11, November 2017

## 6.1. Health Operation

Several tests have been performed to check the accuracy of the proposed model in the first step, the DFIG is tested and simulated in a healthy operation with a rotor speed of 1440 rpm. The wind speed applied to the machine then active and reactive power developed as shown in Figures6-11.

t (s)	0	4	7
V(m/s)	12	14	13
Qsref (var)	0	0	0

Table 1: Variation of wind speed

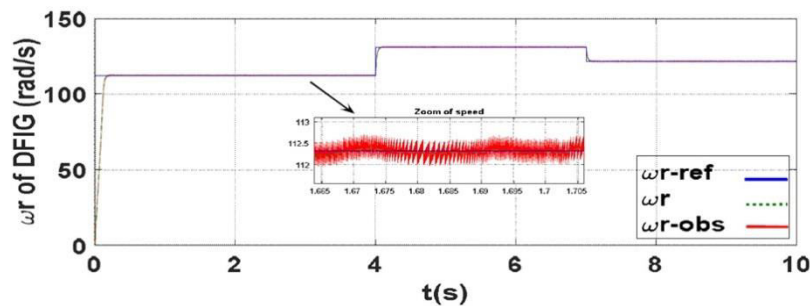


Figure 6: Speed of healthy DFIG and its reference with variation of wind speed.

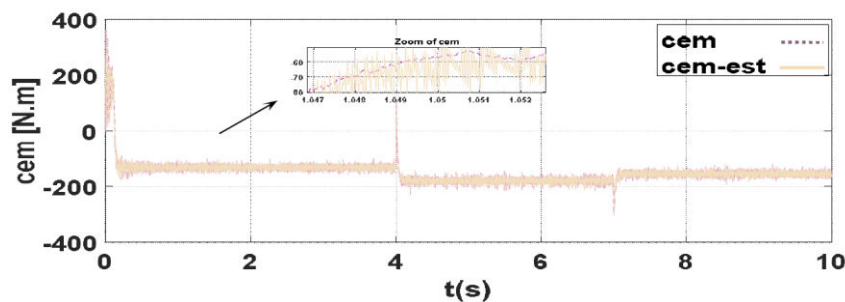
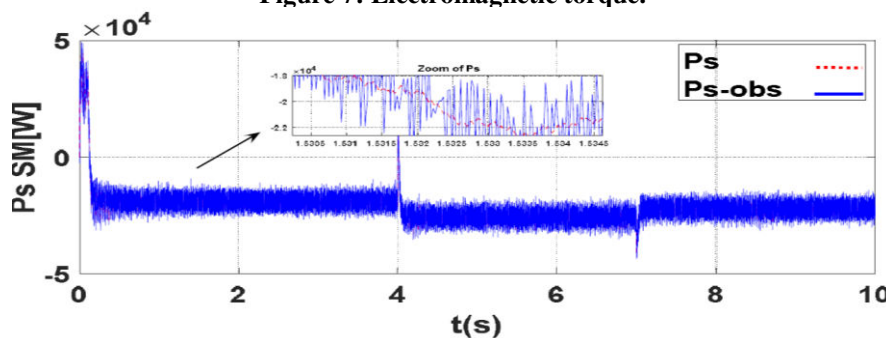


Figure 7: Electromagnetic torque.



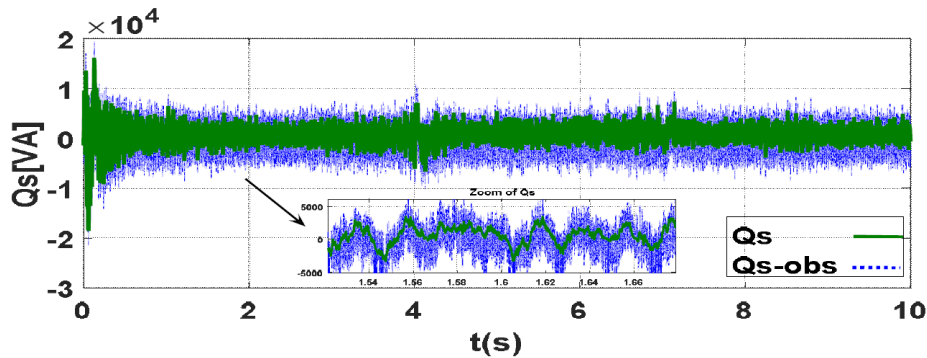


Figure 8: Stator active and reactive powers of healthy DFIG with wind speed variation.

## 6.2. Inter-turn Stator Fault Operation of the DFIG

In this part, we present simulation results for the DFIG operation with stator inter-turn short circuit fault. The inter-turn fault is introduced in winding of stator phase "a". The degree of short-circuit and the time of its application is presented in Table 2.

t (s)	0	1
g (%)	0.1	5

Table 2: Degree of short-circuit and the time of its application.

We present simulation results for the DFIG operation with stator inter-turn short circuit fault. The inter-turn fault is introduced in winding of stator phase "a". We note that the performances of DFIG reduced when the increase of the fault degree that influences on the equilibrium of the three stator phases and therefore the equilibrium of the stator currents which affects the power output, this increase is due to the presence of short-circuit fault. Their responses present a deformations after augmentation of stator and rotor short-circuit fault degree to 5% à time t=1s.

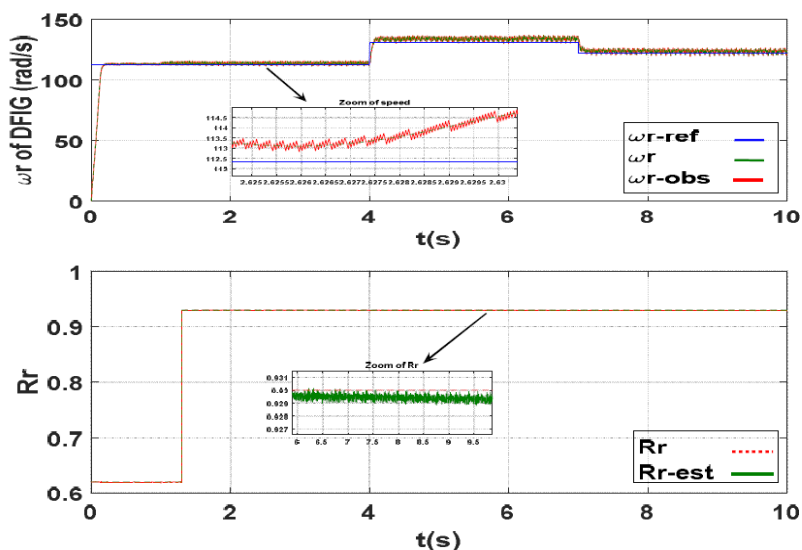


Figure 9: Rotation speed and observed rotor resistance of the DFIG.

# International Journal of Advanced Research in Electrical, Electronics and Instrumentation Engineering

(An ISO 3297: 2007 Certified Organization)

Website: [www.ijareeie.com](http://www.ijareeie.com)

Vol. 6, Issue 11, November 2017

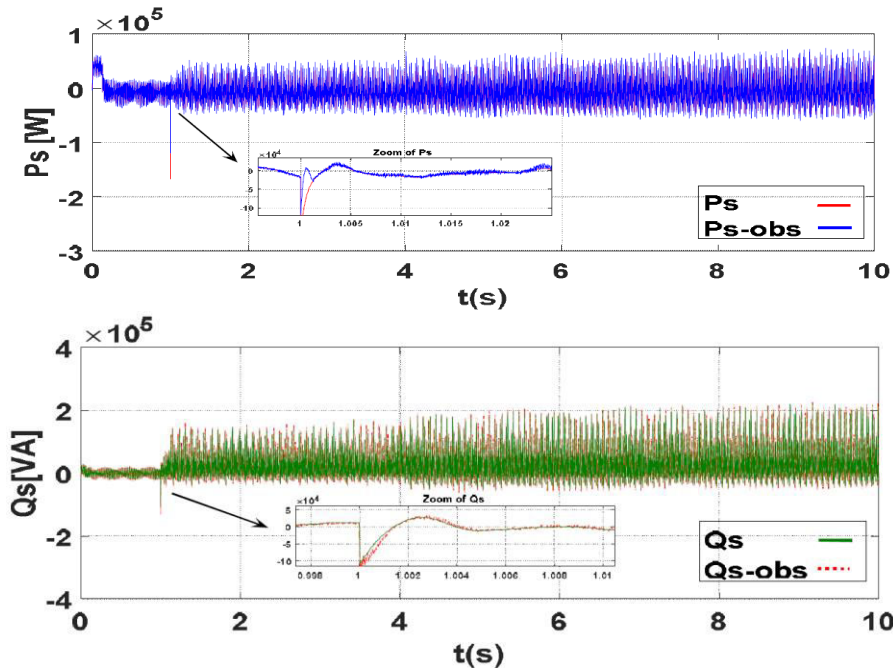


Figure 10: Stator reactive and active powers of faulty DFIG with wind speed variation.

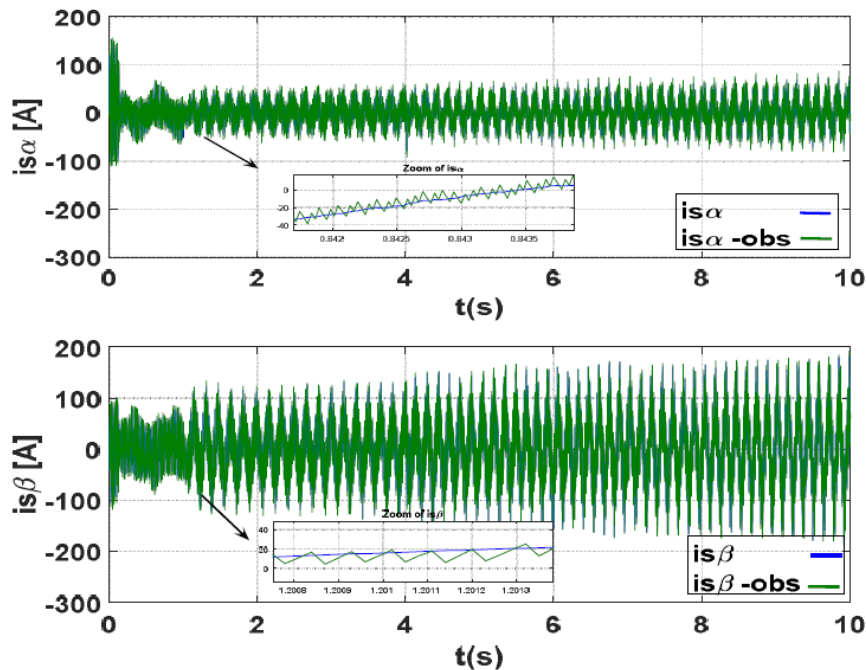


Figure 11: Stator phase current of healthy DFIG and its zoom with speed wind variation.



# International Journal of Advanced Research in Electrical, Electronics and Instrumentation Engineering

(An ISO 3297: 2007 Certified Organization)

Website: [www.ijareeie.com](http://www.ijareeie.com)

Vol. 6, Issue 11, November 2017

## VII. CONCLUSION

In this paper a new method has been presented to modeling of doubly-fed induction generator (DFIG) based wind turbine, and a new scheme of sliding mode observer of Double Fed Induction Generator, based on the estimation of the value of the rotor resistance. The estimation of the rotor resistance is based on the use of the error between real and estimated value of DFIG in faulty condition, this will have to improve the performances of robustness and stability and precision for the sliding mode observer. The results show that the proposed, even in presence of rotor resistance variation. The FTC control strategy has been validated steady-state conditions by Matlab/simulink.

### Wind Turbine Parameters

Rated power:  $P_s = 7500\text{W}$

Moment of the inertia:  $J = 0.31125\text{ kg.m}^2$

Wind turbine radius:  $R = 3\text{m}$

Gear box ratio:  $G = 5.4$

Air density:  $\rho = 1.25\text{ kg/m}^3$

### DFIG Parameters

Rated power:  $7500\text{W}$

Mutual inductance:  $L_m = 0.0078\text{ H}$

Stator leakage inductance:  $L_s = 0.0083\text{ H}$

Rotor leakage inductance:  $L_r = 0.0081\text{ H}$

Stator resistance:  $R_s = 0.455\ \Omega$

Rotor resistance:  $R_r = 0.62\ \Omega$

Number of pole pairs:  $P = 2$

Moment of the inertia:  $J = 0.31125\text{ kg.m}^2$

Viscous friction:  $f_v = 0.00673\text{ kg.m}^2.\text{s}^{-1}$

## REFERENCES

- [1] Kouchih D, Tadjine M, Boucherit MS, Analysis of controlled induction motor drives with stator faults, International Symposium on Environment Friendly energies and Applications, Northumbria university, Newcastle upon Tyne, United Kingdom 2012.
- [2] Kouchih D, Hachelaf R, Boumalha N, Tadjine M, Boucherit MS, Vector fault tolerant control of induction motor drives subject to stator interturn faults. The 16th Power Electronics and Motion Control Conference and Exposition, Antalya, Turkey 2014.
- [3] Amirat Y, Benbouzid MEH, Ahmar EL, Bensaker B, Turri S. A brief status on condition monitoring and fault diagnosis in wind energy conversion systems. Renewable and Sustainable Energy Reviews 2009; 13: 2629-2636.
- [4] Casadei D, Yazidi A, Diagnostic Technique based on Rotor Modulating Signals Signature Analysis for Doubly Fed Induction Machines in Wind Generator Systems. IEEE Industry Applications Conference 2006; pp. 1525-1532.
- [5] Benbouzid MEH, Review of induction motors signature analysis as a medium for faults detection. IEEE Trans. on Industrial Electronics 2000; 47: 984-993.
- [6] Ebrahimkhani S, Robust fractional order sliding mode control of doubly-fed induction generator – based wind turbines. ISA Transactions 2016.
- [7] Benbouzid MEH, Bibliography on induction motors fault detection and diagnosis. IEEE Trans. on Energy Conversion 1999; 14: 1065- 1074.
- [8] Ghennam T, Berkouk EM, François B, Modeling and control of a doubly fed induction generator (DFIG) based wind conversion system. International Conference on Power Engineering, Energy and Electrical Drives 2009.
- [9] C Wei, ZZhang, Stator Current-Based Sliding Mode Observer for Sensorless Vector Control of Doubly-Fed Induction Generators. IEEE Transactions 2015; 978: 4673-7151.
- [10] Zheng X, Song R, Full order terminal sliding mode stator flux observer for DFIG. IEEE Trans. on Application, 2016; 978: 4673-8644.
- [11] Gritli Y, Stefani A, Filippetti A, Chatti A, Stator fault analysis based on wavelet technique for wind turbines equipped with DFIG, IEEE International Conference on Clean Electrical Power 2009.
- [12] Dinkhauser V, Friedrich W, Detection of Rotor Turn-to-Turn Faults in Doubly-Fed Induction Generators in Wind Energy Plants by means of Observers 2009.
- [13] Ur Rehman A, Yu Chen, Simulation using MATLAB/Simulink on Rotor Winding Inter-turn Short Circuit Fault in DFIG 2016.
- [14] Thomsen JS, Kallesoe CS, Stator fault modeling of induction motors, IEEE Int. Symposium on Power Electronics, Electrical Drives, Automation and Motion 2006; 1275-1280.
- [15] Abadi MB, Cruz SMA, Gonçalves AP, Mendes AMS, Ribeiro A, et al. Inter-turn fault detection in doubly-fed induction generators for wind turbine applications using the stator reactive power analysis. Department of Electrical and Computer Engineering 2014.
- [16] Zafar J, Gyselinc J, CUSUM based Fault Detection of Stator Winding Short Circuits in Doubly-Fed Induction Generator based Wind Energy Conversion Systems. Department of Electrical Engineering, Université Libre de





ISSN (Print) : 2320 – 3765  
ISSN (Online): 2278 – 8875

# International Journal of Advanced Research in Electrical, Electronics and Instrumentation Engineering

*(An ISO 3297: 2007 Certified Organization)*

Website: [www.ijareeie.com](http://www.ijareeie.com)

**Vol. 6, Issue 11, November 2017**

Bruxelles2010.

[17] Kia MY, Hybrid modelling of doubly fed induction generators with inter-turn stator fault and its detection method using wavelet analysis. Department of Power Engineering, Faculty of Engineering, University of Birjand Iran 2013.

[18] Lu Q, Breikin T, Wang H, Modelling and Fault Diagnosis of Stator Inter-Turn Short Circuit in Doubly Fed Induction Generators. Control System Centre, School of Electrical and Electronic Engineering the University of Manchester 2011.

[19] Zafar J, Winding Short-Circuit Fault Modelling and Detection in Doubly-Fed Induction Generator based Wind Turbine Systems. Phd Thesis, Université libre de Bruxelles, Faculty of Applied Sciences Department of Electrical Engineering 2011.

[20] Douglas H, Pillay P, The detection of inter-turn stator faults in doubly-fed induction generators. In Proceedings of IEEE Industry Applications Conference 2009; 1097-1102.